Active and Passive Elec. Comp., 2000, Vol. 23, pp. 75–95
Reprints available directly from the publisher
Photocopying permitted by license only

THE POTENTIAL OF REACTIVELY RF SPUTTERED ZnO THIN FILMS FOR THE FABRICATION OF MICROWAVE FILTERS

A. T. KOLLIAS, E. D. TSAMIS and J. N. AVARITSIOTIS*

Department of Electrical and Computer Engineering,
National Technical University of Athens, 9, Iroon Polytechniou St. Zografou,
Athens, 15773, Greece

(Received 20 April 2000; In final form 25 April 2000)

The piezoelectric properties of reactively sputtered ZnO thin films deposited on glass and silicon substrates were studied in order to assess their potential for the construction of RF overmoded filters. Films of high crystallographic orientation {002}, as shown by XRD measurements and SEM observations, and high value of k^2_{eff}, calculated with the aid of the BVD model, were obtained after the optimization of the deposition conditions, with highly repetitive properties. Simple devices were designed and constructed on silicon substrates which showed a quality factor of 1000 without the use of a Bragg acoustic reflector, and a temperature drift of -30 ppm/°C.

Keywords: Zinc oxide; Overmoded resonator; Piezoelectric filters; BAW

1. INTRODUCTION

Zinc oxide (ZnO) thin films are extremely promising as electro-mechanical elements for use with micromechanical structures given that ZnO is a semiconductor with a high piezoelectric coupling factor.

ZnO films have up to now been used mainly in sensing applications. For example, Itoh and Suga [1] have reported on the development of

*Corresponding author. e-mail: abari@cs.ntua.gr

a force sensor for atomic force microscopy (AFM) using ZnO films deposited by r.f. magnetron sputtering. Deschanvres *et al.* [2] have investigated the piezoelectric characteristics of ZnO films, deposited by CVD, as sensors. Blorn *et al.* [3] has reported on the application of ZnO as a micromechanical actuator at low frequencies. They have shown that the fabrication of an actuator as a MOS device produces a piezoelectric actuator suitable for use at low frequencies, since the insulating SiO_2 layer reduces electrical leakage. There are many applications for piezoelectric microactuators such as microoptics [4], linear stepper motors [5], scanning mirror drives [6], microsurgery [7, 8], scanning force microscopy [9], ultrasonic sensor for gas flow measurement [10] and micromechanical cantilevers [11] and flexural actuators [12].

The use of ZnO as a piezoelectric transducer has also been reported for SAW resonators [13] and BAW resonators [14]. Due to wireless communications exponential growth the last years there is increased interest in on-chip thin film resonators (TFRs) for applications in high frequency filters. In particular the majority of heterodyning communication transceivers rely heavily upon the high Q of SAW and BAW mechanical resonators to achieve adequate frequency selectivity and low phase noise and stability [15]. At present the aforementioned devices are off chip components consuming a sizeable portion of the total transceiver subsystem area. Also these required components are a bottleneck to singe chip transceiver fabrication. The construction of TFRs is compatible with the rest of silicon semiconductor processing steps and has the potential to integrate on chip the functions of the aforementioned off chip components [29, 28].

2. ZnO THIN FILM DEPOSITION

ZnO films were prepared using an r.f. sputtering system which was equipped with a horizontal cathode. A detailed description of the sputtering system may be found elsewhere [16]. Typically, the system was pumped down to a base pressure of $1E-6$ mbar before introducing the process gases (Ar_2/O_2). The substrate temperature varied between room temperature and 400°C. ZnO films were deposited onto

glass and {100} silicon wafers covered with a Zn bottom electrode, which was also deposited by r.f. sputtering. ZnO film deposition followed. It is well known that the physical properties of sputtered films are influenced by growth parameters [17–19], such as substrate temperature, sputter gas composition and pressure. Also deposition parameters affect film resistivity [20]. With this in mind, we have optimized sputtering conditions, such as the partial gases pressures temperature and the r.f. input power. Typical sputtering conditions for Zn and ZnO are listed in Table I. The sputtering targets are obtained by casting Zn (purity 99.99%) on Cu target holders. With these conditions the growth rate is of the order 125 Å per min. ZnO films with thicknesses ranging from 1 to 2 μm were deposited. The substrate temperature was varied between room temperature and 400°C. For low and high substrate temperatures the piezoelectric activity of the films degrades appreciably. Below 100°C the films exhibit very poor *c*-axis orientation. In general, the degree of orientation is strongly influenced by the substrate temperature [21].

The ZnO films require upper and bottom electrodes in order for them to be used as piezoelectric devices. Each electrode consisted of a Zn layer of thickness between 0.1 and 0.3 μm. While the bottom electrode run all over the sample surface the top Zn electrodes were patterned using metal contact masks to enable individual dots of various diameters, between 100 μm and 500 μm, to be made. Provision was taken so that close to the individual dots a much larger area ground electrode was deposited. The structure of the final device is shown in Figure 1. This large area ground electrode functions as a low impedance ac conductive path to the bottom electrode to minimize parasitic effects [26].

TABLE I ZnO–Zn deposition parameters

Sample no.	#1	#2	#3
Temp (°C)	Room temp	200	300
Total Pressure (mTorr)		$3E-3$	
Time (hours)		2.5	
Cathode current (A)		0.26	
H.T. (kV)		1.4	
DC Potential (Volt)		220	
Ar_2/O_2 (ZnO desposition)		20 (ml/min)/30 (ml/min)	

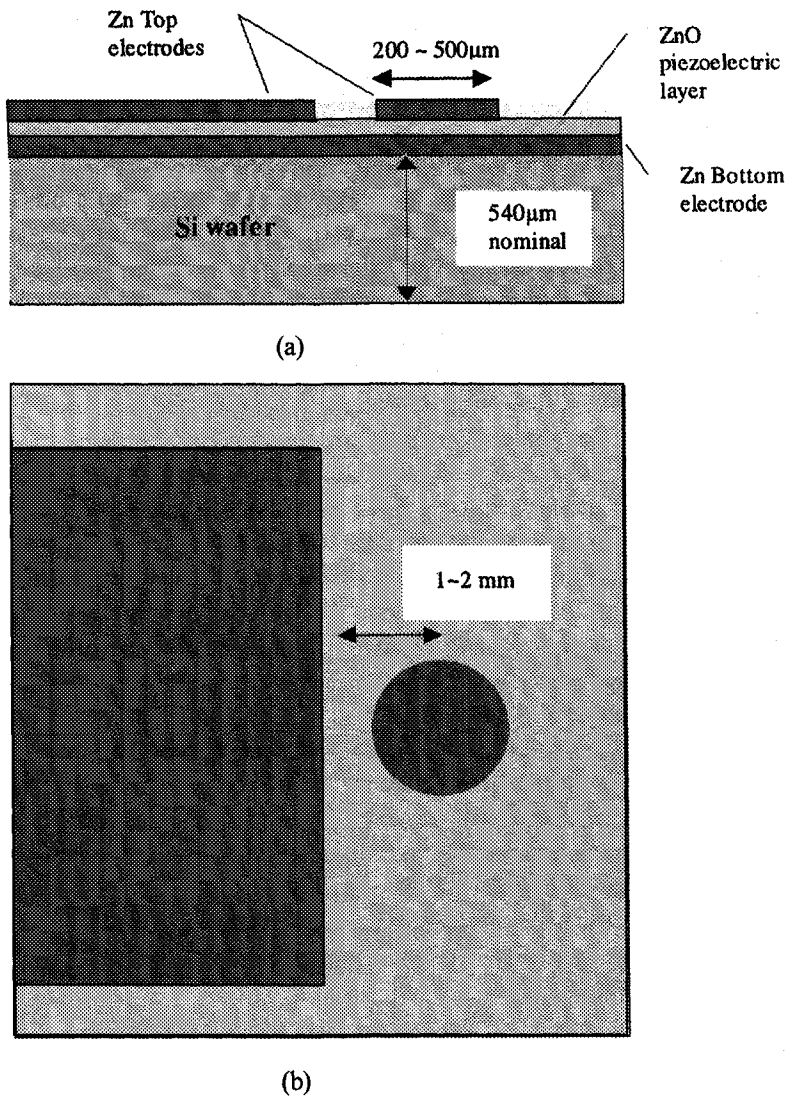

FIGURE 1 Cross section (a) and top view (b) of the device used for piezoelectric film high frequency measurements (Not in scale).

3. FILM CRYSTALLOGRAPHIC ORIENTATION

Sputtered ZnO thin films are generally polycrystalline with a *c*-axis preferred orientation [10]. The intensity of the {002} peak is a direct

indication of the *c*-axis orientation perpendicular to the substrate surface. Film orientation is shown by XRD spectra in Figures 2–4 for films grown at different substrate temperatures. The {002} peak intensity increased by a factor of more than two when the substrate temperature was increased. The crystallinity improved as the growth temperature increased, as shown by the X-ray diffraction peak intensity and its width. The microstructure of the ZnO films was observed using scanning electron microscopy (Fig. 5). This observation showed that the structure is dense and minimal porosity. No cracks or voids were present. The oriented films have a

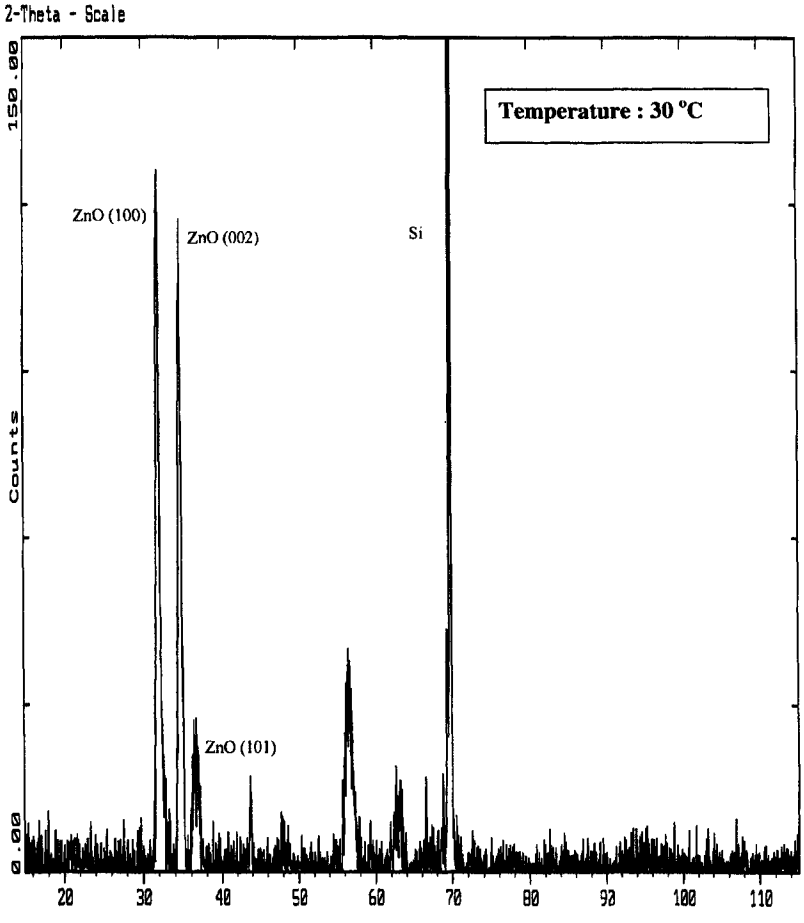

FIGURE 2 XRD spectra obtained from ZnO film deposited at 30°C.

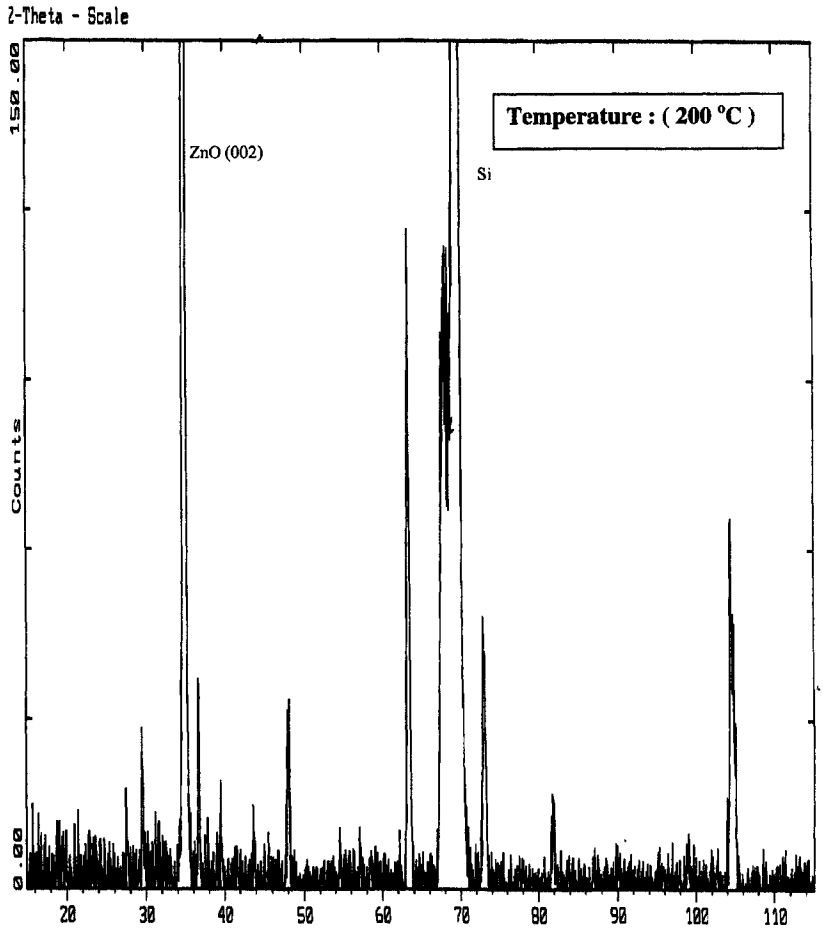

FIGURE 3 XRD spectra obtained from ZnO film deposited at 200°C.

columnar structure with columns perpendicular to the substrate. The primary effect of a change in composition from an oxygen-deficient material to stoichiometric ZnO is a preferred {002} orientation. Since no other peaks besides the {002} orientation where present at 200°C deposited films these are thought to be nearly stoichiometric.

An increase in the preferred {002} orientation with increasing O_2, pressure in the Zn/ZnO film has been observed. It may be

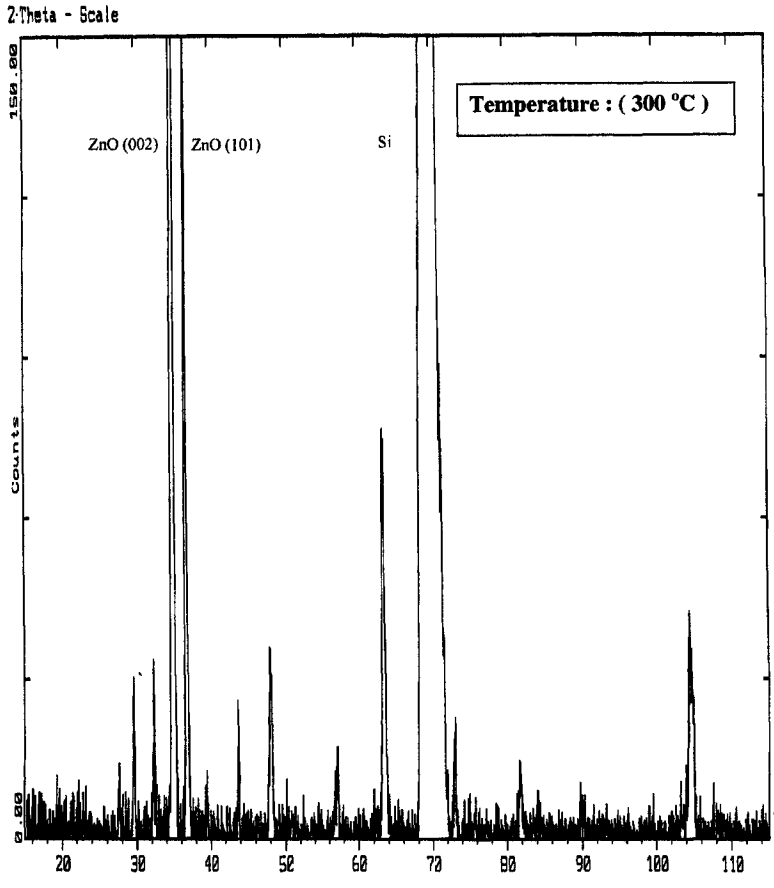

FIGURE 4 XRD spectra obtained from ZnO film deposited at 300°C.

argued that the variation in the ZnO crystal structure, is due to the competing effects of ion bombardment causing film amorphization and the increased oxygen content in the sputtering gas mixture causing improved crystallinity and a preferred {002} orientation. The resputtering of the films by high-energy neutral oxygen atoms is thought to be dominant because the sputtering pressure was set to $3E-3$ mTorr in this study. Therefore, the observed decrease in the preferred {002} orientation with decreasing Ar_2/O_2, ratio can be explained by the resputtering effect of the neutral oxygen [22].

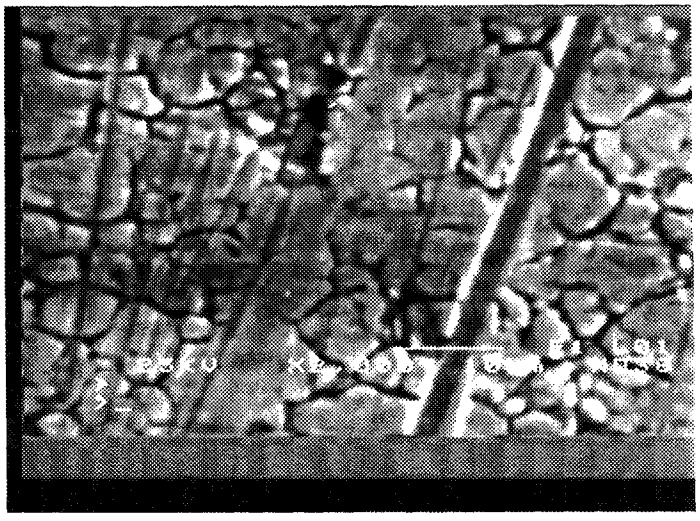

FIGURE 5 SEM photograph of ZnO film surface.

4. METHODS FOR MEASURING THE PIEZOELECTRIC PROPERTIES

4.1. Static Methods

In general the electrical properties of a piezoelectric material in thin form can be determined by static methods and dynamic ones. Static methods [23, 24] are straight forward to use. Using the direct piezoelectric effect (dp) by applying a stress and measuring the induced charge (or voltage), or by use of the inverse piezoelectric effect (ip), *i.e.*, applying a voltage (electric field) and measuring the induced elongation (strain). In principle, both methods allow to measure the piezoelectric coefficient d_{33} called charge constant. It is defined by:

$$d_{33} = \left(\frac{\partial S_3}{\partial E_3}\right)_T \quad \text{or} \quad d_{33} = \left(\frac{\partial D_3}{\partial T_3}\right)_E \tag{1}$$

where S is the strain, E the electric field, D the electric displacement, and T the stress in the appropriate direction.

In the normal load method, a weight is applied on an area A of the piezoelectric film and the induced charge, stored in a capacitor

connected across the piezoelectric device, is measured. The accuracy of this method is limited by electric leakage through the capacitors (leading to a decrease of the induced charge) and by electric noise. However, the method can be very easily implemented to determine d_{33} (ip) of thin films.

A high input impedance voltmeter was needed to measure the voltage over the capacitor. It was checked that the piezoelectric effect was reversible, *i.e.*, that increasing or decreasing the force led to opposite voltages. It was also verified that the induced voltage increased linearly with force and d_{33} was calculated from the slope of this line. This linear relationship conforms to the piezoelectric theory since the measurements were done in the low signals region (stress less than 20 MPa).

The use of aforementioned static methods gave us an easy tool to make preliminary comparative studies between samples prepared at different deposition conditions in order to discover the optimum deposition conditions required for the ZnO thin films.

4.2. Dynamic Methods

Consequently, a dynamic method was employed in order to study the potential of ZnO films for the fabrication of high frequency filters. The most important parameter for thin piezoelectric film high frequency applications is the electromechanical coupling factor K^2. The calculation of this term from material piezoelectric elastic and dielectric parameters varies for different film excitation and boundary conditions. The bandwidth of piezoelectric filters and transducers is dependent upon the appropriate coupling factor. Different materials can directly be compared for the same application from their coupling factors without knowledge of their sets of elastic dielectric and piezoelectric constants [25]. In high frequency filters (GHz range) the thickness of the film is only a few microns with much larger lateral dimensions so a film supporting structure is required. The film with the necessary electrodes and the supporting substrate form a composite structure known as overmoded resonator with the substrate acoustic properties (mechanical impedance, acoustic losses and surface finish) strongly affecting the measurements of thin film parameters. The one dimensional theory [26] gives the electrical impedance between the

electrodes as:

$$Z_{\text{in}} = \frac{1}{j\omega C}\left[1 - \frac{K^2}{1+K^2}\frac{\tan\theta}{\theta} \cdot \frac{(z_{\text{above}} - z_{\text{below}})\cos^2\theta + j\cdot\sin(2\cdot\theta)}{(z_{\text{above}} - z_{\text{below}})\cos(2\cdot\theta) + j(1 - z_{\text{above}}\cdot z_{\text{below}})\sin(2\cdot\theta)}\right] \tag{2}$$

with the electromechanical coupling factor defined as:

$$K^2 = \frac{e^2}{c^E \varepsilon^S} \tag{3}$$

where e, c^E, and ε^S are the piezoelectric stress constant, stiffness constant at constant E and dielectric constant at constant strain respectively.

$$\theta = \frac{kd}{2} \tag{4}$$

is half the phase delay in the piezoelectric layer and z_{above}, z_{below}, are the mechanical input impedances above and below the piezoelectric film respectively normalised with the mechanical impedance Z_p of piezoelectric film. At each material interface the input impedance is calculated using a transmission line model. For example the input impedance at the interface piezoelectric film/bottom Zn electrode is:

$$Z_{\text{in, Zn}} = Z_{\text{Zn}}\left(\frac{Z_{\text{in, Si}}\cos(-\vartheta) + jZ_{\text{Zn}}\sin(-\vartheta)}{Z_{\text{Zn}}\cos(-\vartheta) + jZ_{\text{in, Si}}\sin(-\vartheta)}\right) \tag{5}$$

where Z_{zn} is the Zinc characteristic impedance $Z_{\text{in, Si}}$ the input mechanical impedance at the Zinc/Silicon interface and ϑ the phase delay in the bottom electrode. The theory does not take account of acoustic wave diffraction taking place inside the substrate giving substantial additional losses. In the input electrical impedance formula the effect of the electrodes (thickness $< 0.3\,\mu\text{m}$) is usually neglected and the losses are mainly due to wave propagation in the much thicker substrate. Losses can be introduced through a complex material stiffness

$$c = c_{\text{real}} + 2\pi f\eta \tag{6}$$

where f is the frequency and η the acoustic viscosity. The Sitting's model [27] of a piezoelectric transducer attached between a backing and a transmitting medium can also be used to obtain the same relation for input impedance given by Eq. (2).

A simulated electrical input impedance for an overmoded resonator on a {100} silicon substrate is given in Figures 6(a)–(c) with data in Table II.

The equation describing an ideal thin film resonator electrical input impedance is a good reference for understanding the overmoded resonator:

$$Z_{\text{ideal, TFR}} = \frac{1}{j\omega C}\left[1 - \frac{K^2}{K^2+1}\frac{\tan\varphi}{\varphi}\right] \tag{7}$$

where C is again the clamped capacitance K^2 the coupling factor and φ the half the phase delay in the piezoelectric film. In the above relation the electrodes are ideal, with zero thickness and

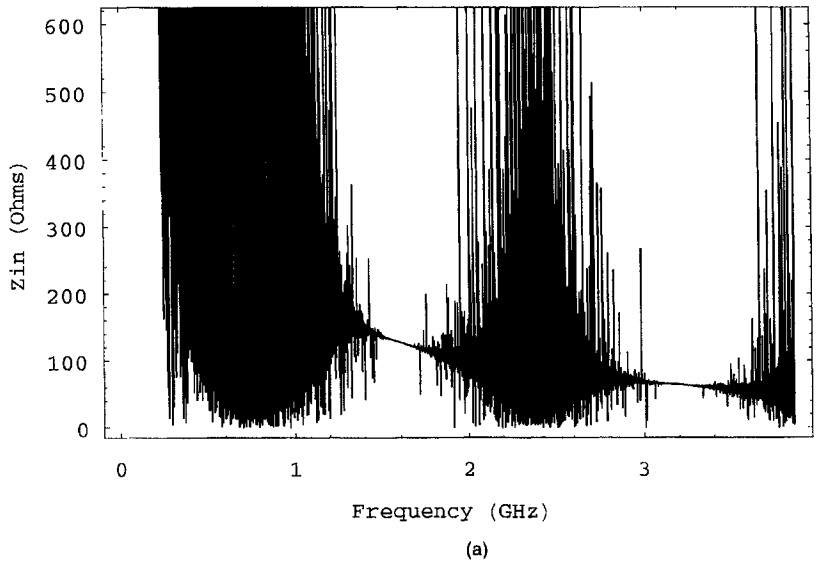

FIGURE 6 Simulated response for an overmoded resonator based on the data from Table II. (a) Broad band impedance magnitude, (b) Impedance magnitude near a single resonance, (c) phase response for (b), and (d) ideal TFR's impedance magnitude.

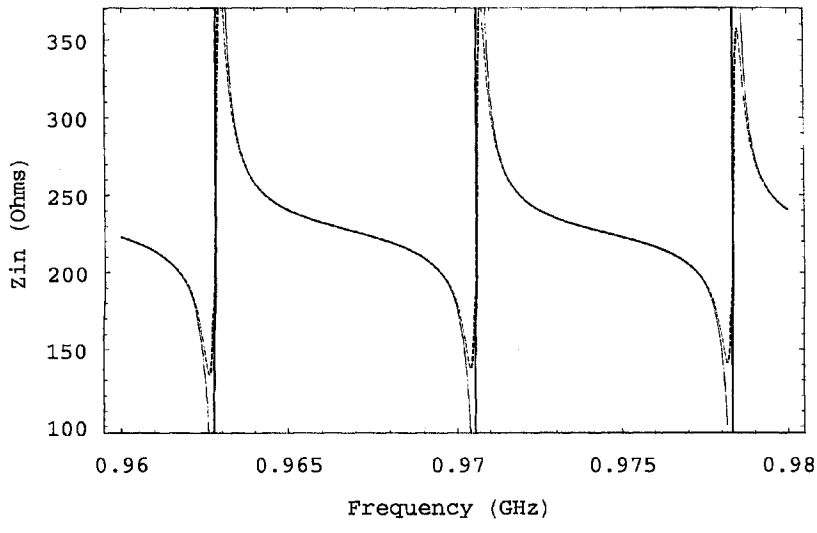

(b)

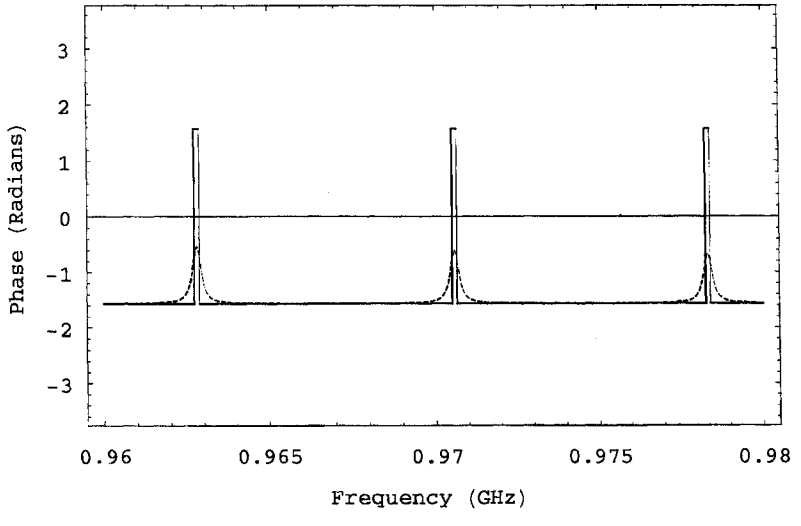

(c)

FIGURE 6 (Continued).

$Z_{\text{above}} = Z_{\text{below}} = 0$. Comparing Eq. (2) with Eq. (7) we see that Eq. (2) contains Eq. (7) so the overmoded resonator response is a modulated ideal resonator response with substrate introducing a

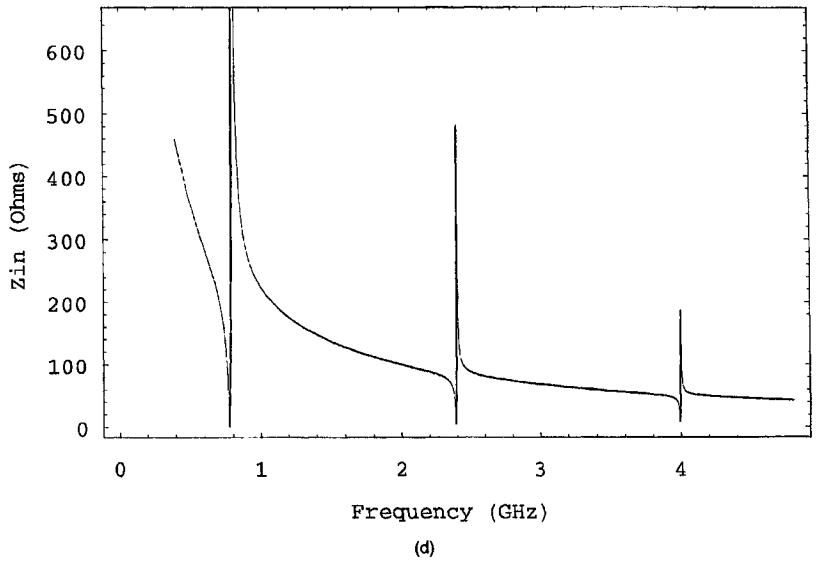

(d)

FIGURE 6 (Continued).

TABLE II Data for the simulated response of an overmoded resonator seen in Figure 6

Layer	*Thickness* l_i (μm)	*Density* ρ_i (Kgr/m^3)	*Stiffness* ($Nt/m^2 \times 10^9$)	*Viscosity* n ($(Nt \cdot sec)/m^2$)	*Comments*
ZnO	4.0	5675	232.5	–	The solid line in Figure 6 is with Si $n = 0$ and the dashed with $n = 0.008$
Si {001}	540	2332	165.7	0.008	

multiplicity of short spaced resonances on the wide separated and few of the ideal thin film resonator also seen in Figure 6(d).

Each resonance seen in Figure 6(b) can be quantified by two figures of merit k^2_{eff} the effective coupling constant and Q the quality factor. These are defined as:

$$k^2_{\text{eff}} = \frac{(\pi/2)(f_s/f_p)}{\tan((\pi/2)(f_s/f_p))} \tag{8}$$

$$Q = \frac{f_s}{2}\frac{\partial \angle Z}{\partial f}\bigg|_{f_s} \tag{9}$$

where f_s, f_p are the frequencies at which the magnitude of impedance is minimum and maximum respectively.

The first term k_{eff}^2, is a strong function of the electromechanical coupling factor K^2, Q is independent of k_{eff}^2 and expresses the material losses. Because the overmoded resonator suffers from excess loss the calculation of these terms directly from the measured response is inaccurate. On the contrary for low loss resonators such as crystal resonators in the MHz range the above equations are directly applicable.

4.3. The BVD Model

A method for indirectly obtaining the aforementioned figures of merit is described in [28]. It is based on the the Butterworth-Van Dyke (BVD) equivalent circuit (Fig. 7). The electrical input impedance of the BVD circuit is calculated as:

$$Z = \left(\frac{1}{j\omega(C_1 + C_2)}\right) \frac{1 - (f/f_s)^2 + (j/Q_s)(f/f_s)^2}{1 - (f/f_p)^2 + (j/Q_p)(f/f_p)^2} \tag{10}$$

with

$$f_s = \frac{1}{2\pi}\sqrt{\frac{1}{LC_1}}, \quad f_p = \frac{1}{2\pi}\sqrt{\frac{C_1 + C_2}{LC_1C_2}}, \quad Q_{\text{BVD}}|_{s,p} = \frac{2\pi f_{s,p} L}{R} \tag{11}$$

In the neighbourhood of a single resonance of the overmoded resonator its response is similar to the response of the BVD circuit shown in Figure 7. By varying the parameters of the BVD circuit we can fit the two responses. At the condition of best fit according to some

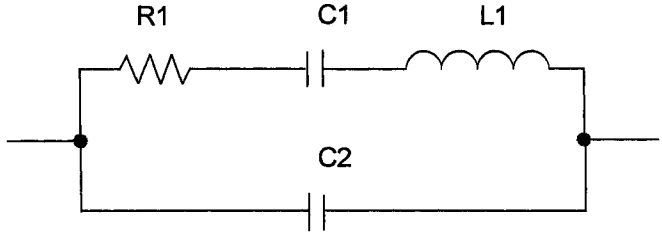

FIGURE 7 The electrical equivalent circuit for the BVD model of a lossy resonator.

cost criterion (such as least squares) we use the BVD circuit element values for the calculation of piezoelectric film's figures of merit. The k^2_{eff} of the resonator is calculated from the f_s, f_p of the BVD model and Eq. (7). In the model two values Q_s and Q_p for the quality factor appear. These values approach a common value as frequency increases. The fitting of the two responses can be done either from phase or magnitude data but it was found that phase fitting gives better results.

5. EXPERIMENTAL RESULTS FROM THE RESONATORS

5.1. Measuring Techniques

All measurements were done on an HP8753D network analyser and a home-made microwave probe station at different temperatures. Silicon wafers having nominal thicknesses of 540 μm optically polished in one side were used as substrates. Zn/ZnO/Zn structures were tested being fabricated on both the polished and the rough wafer face. The resonators consisted of zinc oxide *c*-axis normal films with circular electrodes of $\sim 0.3\,\mu$m thick zinc as shown in Figure 1. The ZnO thickness was calculated to induce resonance in the center of the frequency range of interest for maximum excitation efficiency. Silicon was chosen as the primary substrate material during these initial investigations because of its known high Q and ready availability in optically polished wafers. Glass substrates with nominal thickness 150 μm were also used, but with surface parallelism inferior to the silicon substrates. Also due to amorphous nature of glass material losses were much higher giving very weak resonator responses.

The calculated Q_s, Q_p and K^2_{eff} are tabulated in Table III for polished and unpolished Si wafer backside at different deposition temperatures. The XRD results for these films are given in Figures 2–4, respectively.

5.2. Effective Piezoelectric Coupling Factor

The first observation is that the substrate surface roughness affects the coupling factor with much lower coupling factor for deposition in a

TABLE III The calculated Q_s, Q_p and K^2_{eff} from measured S11 data. The piezoelectric ZnO films where deposited at various temperatures

Backside	*Resonator sample no.*	*Temp* (°C)	f_s (*MHz*)	f_p (*MHz*)	Q_s	Q_p	K^2_{eff} ($\times 1E-3$)	*Comments*
Polished	1	300	301.8	302.0	368	498	2.12	
	2	200	269.9	270.1	517	497	1.88	
	3	20	–	–	–	–	–	Very weak S11 response
Unpolished	4	200	238.7	230.3	100	142	17.10	
	5	20	–	–	–	–	–	Very weak S11 response

rough surface. This is seen by comparing the 200°C temp K^2_{eff} data on Table III on a polished and unpolished surface wafer.

The network analyser measurements verify that the resonators present maximum performance at substrate temperature of 200°C. From Table III one can see that the calculated K^2_{eff} is an order of magnitude greater for these films. This was expected because films, deposited at 200°C temperature, feature only a strong {002} preferred orientation. On the other hand for higher deposition temperatures (300°C) the {101} orientation becomes relative strong reducing K^2_{eff} and inducing spurious resonances observed for small lateral dimension resonators. For film deposition at room temperature the films show many crystallographic orientations of the same small size verified by the weak and full of spurious S11 network analyzer rmeasurements.

5.3. Quality Factor

The overmoded resonator quality factor Q_s, Q_p calculated from the experimental results depends strongly on the finish of wafer backside and it is independent of piezoelectric film's coupling factor. This is expected because acoustic scattering in an unpolished wafer backside reduces greatly the energy reflected toward the piezoelectric transducer lowering the Q of the device. The rest of the scattered energy is attenuated inside the Si wafer.

Spurious resonances were observed and become very pronounced if the overall structure, including the device, had nonparallel surfaces or the lateral dimensions of the resonator were relatively small. Also in the high temperature samples the non perfect film orientation with the strong {101} peak induced spurious resonances who where cancelled out in larger lateral dimensions resonators.

5.4. Working Temperature Effects

The "best" of the above resonators were tested at various temperatures. S11 plot *versus* frequency for mode number 34 and 35 at temperatures 30 and 100°C is shown in Figure 8.

The results for mode number 35 are tabulated in Table IV. As seen the calculated f_s, f_p varies slightly with temperature. The temperature coefficient which is of the order of -30 ppm/°C comparable with the

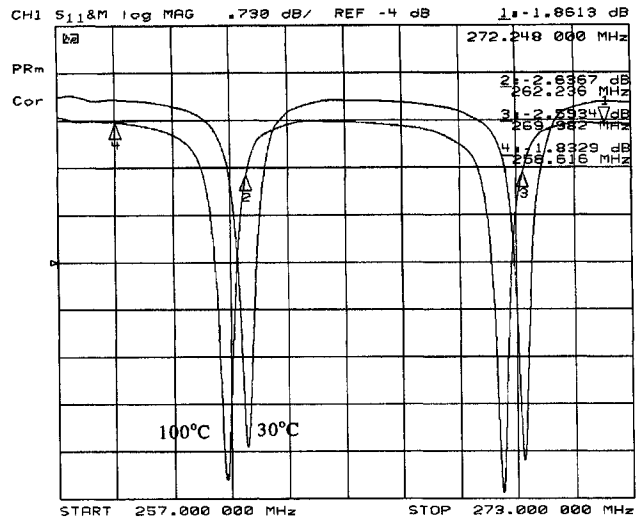

FIGURE 8 Overmoded resonator S11 response at 30°C and 100°C.

TABLE IV The calculated figures of merit at various temperatures for an ZnO overmoded resonator

Temp (°C)	f_s (*MHz*)	f_p (*MHz*)	Q_s	Q_p	k^2_{eff} ($\times 10^{-3}$)
30	269.87	270.11	456	466	2.107
100	269.29	269.54	450	448	2.273
Temp coefficient (ppm/°C)	−30.8	−30.2	−189.2	−252.8	270.1

thermal coefficient of expansion in the order of 10−15 ppm/°C for most materials. This suggests that thermal expansion is the main reason for temperature variation. Also small changes in materials elastic parameters with temperature may contribute to the above change.

It is also interesting to note that the Q of the device drops with temperature. This is attributed to the Akhieser mechanism [28] which predicts a very linear relation between the material attenuation factor α and working temperature. Finally, the observed increase of K^2_{eff} with working temperature is due to thermal expansion of the piezoelectric layer. As its thickness approaches the $\lambda/2$ value where λ is the piezoelectric material's acoustic wave length at the specified frequency the coupling between the electromagnetic and acoustic fields

becomes maximum thus K^2_{eff} increases. However, if piezoelectric layer's thickness was larger than $\lambda/2$ a reduction with temperature would be observed.

6. CONCLUSIONS

The results of the present study show that reactively sputtered ZnO thin films are very good candidates for the construction of overmoded TFR filters to be used at the RF part of the spectrum. To this contribute the easiness of deposition of highly oriented films and the repeatability of the process together with the recorded low temperature drift that does not exceed, in our case the value of $-30\,\text{ppm/°C}$.

The quality factor Q, of our devices is close to 1000 without any attempt to increase it further, by the use possibly of a Bragg acoustic reflector, since it was outside the scope of this work.

It is expected that the use of several devices, as the ones studied in this work, in a ladder interconnection and with the proper ZnO thickness will allow the construction of tailored bandpass overmoded filters.

References

[1] Itoh, T. and Suga, T. (1993). Development of a force sensor for atomic force microscopy using piezoelectric thin films, *Nanotechnology*, **4**, 218–224.

[2] Deschanvres, J. L., Rey, P., Delabot~glise, G., Labeau, M., Joubert, J. C. and Peuzin, J. C. (1992). Characterization of piezoelectric properties of zinc oxide thin films deposited on silicon for sensors applications, *Sensors and Actuators A*, **33**, 43–45.

[3] Blom, F. R., Yntema, D. J., Van de Pol, F. C. M., Elwenspoek, M., Fluitman, J. H. J. and Popma, Th. J. A. (1990). Thin-film ZnO as micromechanical actuator at low frequencies, *Sensors and Activators*, **A21**, **A23**, 226–228.

[4] Motamedi, M. E. (1994). Micro-opto-electro-mechanical systems, *Opr. Erg.*, **33**, 3505–3517.

[5] Judy, J., Polla, D. L. and Robbins, W. P. (1990). A linearpiezoelectric stepper motor with sub-micron step size and centimeter travel range, *IEEE Trans. Ultrasonics*, Ferroelectrics Freq. Control, **37**, 428–437.

[6] Tominanga, T., Ohya, N., Senda, K., Idogaki, T. and Hattori, T., Flexible stacked type actuators, *Proc. 5th Int. Sytnp. Micro Machine and Hctman Science (IEEE) 1994*, pp. 143–147.

[7] Miyazaki, H., Kameya, T., Sato, T., Hatamura, Y. and Morishita, H., Construction of an ultra-micro manipulation system based on visual control-realisation of nano-hand-eye system, *IEEE Symp. Emerging Technologies Factory Autornation 1994*, pp. 74–77.

[8] Menz, W. (1993). Three-dimensional microstructures in various materials for medical applications, *Int. Conf. Systems, Man and Cybernetics*, pp. 417–422.
[9] Cunningham, M. J., Cheng, S. T. and Clegg, W. W. (1994). A differential interferometer for scanning force microscopy, *Meas. Sci. Technol.*, **5**, 1350–1354.
[10] Kiyotaka Wasa and Shigeru Hayakawa (1992). *Handbook of sputter deposition technology*, Noyes Publications, pp. 135–155.
[11] Jenkins, D. F. L., Cunningham, M. J. and Clegg, W. W., The use of piezoelectric films for actuation and control of miniature cantilevers, presented at *1st Eur. Meet. Integrated Ferroelectrics, Nijmegen, Netherlands*, July, 1995, Microelectronic Eng., **29**, 71–74.
[12] McKinstry, S. T., Fox, G. R., Kholkin, A., Muller, C. A. and Setter, N. (1999). Optical fibers with patterned ZnO electrode coatings for flexural actuators, *Sensors and Actuators*, **73**, 267–274.
[13] Shiosaki, T. and Kawabata, A. (1974). Low-frequency piezoelectric transducer applications of ZnO film, *Appl. Phys. Lett.*, **25**, 10.
[14] Ono, S., Wasa, K. and Hayakawa, S. (1977). Surface acoustic-wave properties in ZnO-SiOz-Si layered structure, *Wave Electron.*, **3**, 35.
[15] Clark T.-C. Nguyen, Linda P. B. Katehi and Gabriel M. Rebeiz, Micromachined Devices for Wireless Communications, *Proceedings of the IEEE*, August, 1998, **86**(8), 1756–1767.
[16] Tsiogas, C. D. and Avaritsiotis, J. N., Practical aspects for the use of plasma emission monitoring in reactive magnetron sputtering, April, 1994, *Vacuum*, **45**(4), 1181–1186.
[17] Krupanadhi, S. B. and Sayer, M. (1984). Position and pressure effects in r.f. magnetron reactive sputter deposition of piezoelectric zinc oxide, *J. Appl. Phys.*, **56**, 3308–3312.
[18] Kmpanidhi, S. B., Sayer, M., Assal, K. E., Jen, C. K. and Farrel, G. W. (1984). Fabrication and characterisation of piezoelectric films for SAW and acoustic microscopy, *J. Can. Cerarn. Soc.*, **53**, 28–33.
[19] Mitsuyu, T., Ono, S. and Wasa, I. C. (1980). Structures and SAW properties of R.F. sputtered single crystal films of ZnO on saphire, *J. Appl. Phys.*, **51**, 2464–2470.
[20] Barker, A., Crowther, S. and Rees, D. (1997). Room-temperature r.f. sputtered ZnO for electromechanical devices, *Sensor and Actuators*, **A58**, 229–235.
[21] Jenkins, D. F., Cunningham, M. J., Velu, G. and Remiens, D. (1997). The use of sputtered ZnO piezoelectric thin films as broad-band microactuators, *Sensors and Actuators*, **A63**, 135–139.
[22] Yoon, K. H., Choi, J. W. and Lee, D. H. (1997). Characteristics of ZnO thin films deposited onto Al/Si substrates by RF magnetron sputtering, *Thin Solid Films*, **302**, 116–121.
[23] Lefki, K. and Dormans, G. J. (1994). Measurement of piezoelectric coefficients of ferroelectric thin films, *J. Appl. Phys.*, **76**(3), 1764–1767.
[24] Kim, D., *Method and apparatus for measuring the piezoelectric constant of a thin film type piezoelectric material*, International Patent Application WO98/25150, 11 June, 1998.
[25] Mason, W. P. (1964). *Physical Acoustics Principles and Methods*, Vol. I, part A, Chapter 3, pp. 190–196, Academic Press.
[26] Rajan S. Naik, Lutsky, J. J., Reif, R. and Sodini, Ch. G., Electromechanical Coupling Constant Extraction of Thin-Film Piezoelectric Materials Using a Bulk Acoustic Wave, Jan., 1998, *Resonator IEEE Trans. Ultras. Ferroel. and Freq. Control*, **45**(1), 257–263.
[27] Mason, W. P. and Thurston, R. N. (1972). *Physical Acoustics Principles and Methods*, Vol. XI, Chapter 5, Academic Press.
[28] Rajan S. Naik, Bragg Reflector thin film resonators for miniature PCS bandpass filters, *Ph.D. Thesis*, Dept. of Electrical Engineering and Computer Science, Massachusetts Institute of Technology, Cambridge MA, 1998.

[29] Lutsky, J. J., A sealed cavity thin film acoustic resonator process for RF bandpass filters, *Ph.D. Thesis*, Dept. of Electrical Engineering and Computer Science, Massachusetts Institute of Technology, Cambridge MA, 1997.
[30] Auld, B. A., "*Acoustic fields and waves in solids*", Vols. 1 and 2, Academic Press, 1990.